Comparative Biochemistry and Physiology, Part C 287 (2025) 110063

Contents lists available at ScienceDirect

Comparative Biochemistry and Physiology, Part C

journal homepage: www.elsevier.com/locate/cbpc

Effect of lead on photosynthetic pigments, antioxidant responses, metabolomics, thalli morphology and cell ultrastructure of *Iridaea cordata* (Rhodophyta) from Antarctica

Riccardo Trentin [a,*], Ilaria Nai [a], Sophia Schumann [a], Gianfranco Santovito [a], Emanuela Moschin [a], Luísa Custódio [b], Isabella Moro [a,c]

[a] Department of Biology, University of Padova, Via U. Bassi 58/B, 35131 Padova, Italy
[b] Centre of Marine Sciences, Faculty of Sciences and Technology, University of Algarve, Ed. 7, Campus of Gambelas, 8005–139 Faro, Portugal
[c] Department of Integrative Marine Ecology, Stazione Zoologica Anton Dohrn, Villa Comunale, 80121 Napoli, Italy

ARTICLE INFO

Edited by Martin Grosell

Keywords:
Iridaea cordata
Metal pollution
Photosynthetic pigments
Antioxidant activity
Untargeted metabolomics
Ultrastructure

ABSTRACT

Over the past decades, the concern about lead pollution in marine environments has increased due to its remarkable toxicity, even at low concentrations. Lead is one of the significant contaminants arising from human activities in Antarctica. However, its effects on polar photosynthetic organisms are poorly known. This work aims to evaluate the effects of two different environmental concentrations of lead (10 μg/L and 50 μg/L) on pigment content, antioxidant enzyme activities (catalase, superoxide dismutase, ascorbate peroxidase and glutathione–S–transferase), metabolome, thalli morphology and cell ultrastructure of the red seaweed *Iridaea cordata* (Turner) Bory from Terra Nova Bay (Ross Sea, Antarctica). The results highlighted that lead exposure decreased phycocyanin and phycoerythrin content, starting from 10 μg/L, while induced carotenoid accumulation at 50 μg/L. Catalase, ascorbate peroxidase, and superoxide dismutase activities generally increased after lead exposure and distinct biochemical features were identified in the control and treatment groups. Further lead–related effects on cell ultrastructure comprised floridean starch accumulation and plastoglobuli formation. Overall, our results suggested that the enhanced formation of reactive oxygen species in response to lead altered the photosynthetic pigment pattern, antioxidant defenses, metabolome and ultrastructure of *I. cordata*.

1. Introduction

Despite being considered the last pristine continent on Earth, Antarctica presents traces of different environmental contaminants (Chu et al., 2019). Pollution in this region is primarily associated with local human activities, including sewage outfalls, abandoned dump sites, accidental oil spills, exhaust emissions and tourism, but it is also influenced by non–local sources (Chu et al., 2019; Bargagli, 2008). Indeed, metals and persistent organic pollutants (POPs) can reach Antarctica via Long–range Atmospheric Transport (LRAT) from other continents (Chu et al., 2019; Bargagli, 2008). Elevated levels of metals, such as copper (Cu), lead (Pb) and mercury (Hg), have been measured in Antarctica, where some metals naturally occur due to geological processes, but human activities have exacerbated their concentrations (Chu et al., 2019). While their effects on invertebrates and cryptogams have been extensively studied, little is known regarding the impact of metals on algae (Pinto et al., 2003). Microalgae and seaweeds constitute the basis of the marine food web (Momo et al., 2020), therefore, adverse effects of metals on marine phototrophs might severely affect species at higher trophic levels (Pinto et al., 2003). Thus, monitoring metal levels in Antarctica and studying their effects on local biota is fundamental for environmental protection and species conservation (Koppel et al., 2019). Lead exposure disrupts cellular processes in algae, particularly by impairing photosynthesis. Pb^{2+} ions accumulate in algal tissues and interfere with the photosynthetic processes by displacing essential metal cofactors, such as magnesium in chlorophyll and zinc in enzymes. This displacement reduces photosynthetic efficiency and accelerates chlorophyll degradation (Chang et al., 2023a). This impairment in photosynthesis lowers primary productivity and can have cascading effects throughout the marine food web, impacting herbivores and higher trophic levels (Pinto et al., 2003). Furthermore, Pb exposure potentially induces oxidative stress in algae by generating reactive oxygen species

* Corresponding author.
E-mail address: riccardo.trentin.2@studenti.unipd.it (R. Trentin).

https://doi.org/10.1016/j.cbpc.2024.110063
Received 26 August 2024; Received in revised form 12 October 2024; Accepted 27 October 2024
Available online 29 October 2024

(ROS) such as superoxide radicals, hydrogen peroxide, and hydroxyl radicals (Chu et al., 2019; Pinto et al., 2003; Kaur et al., 2022; Nowicka, 2022). These ROS can damage critical cellular components, including lipids, proteins, and DNA. In response, algae activate antioxidant defense mechanisms, including enzymes like catalase (CAT), ascorbate peroxidase (APX), and superoxide dismutase (SOD) (Chu et al., 2019; Pinto et al., 2003; Kaur et al., 2022; Nowicka, 2022). Despite these protective mechanisms, high or prolonged Pb exposure can overwhelm antioxidant defenses, leading to persistent oxidative damage, impaired growth, and reduced survival adaptation (Collén et al., 2003). Additionally, lead-induced oxidative stress can alter the metabolomic profiles of algae, affecting the synthesis and accumulation of secondary metabolites crucial for cellular protection and adaptation (Zhang et al., 2013). Climate change is expected to amplify the spread and impact of these contaminants. Melting ice and shifting wind patterns can redistribute pollutants, increasing their bioavailability and potentially harming Antarctic ecosystems (Liu et al., 2024). This interaction between pollution and climate change highlights the urgent need for ongoing monitoring and research to predict future impacts and develop effective conservation strategies (Koppel et al., 2019).

The red seaweed, *Iridaea cordata* (Turner) Bory, is an essential species in Antarctic marine ecosystems, representing a food source for marine herbivores, a shelter for several species and a significant primary producer (Foltran et al., 1996; Iken et al., 1997; Miller and Pearse, 1991). Due to its relatively small thalli, *I. cordata* can be easily studied, thereby avoiding problems with varying metal concentrations throughout the thallus (Runcie et al., 2009). Furthermore, *I. cordata* is widely distributed throughout the Antarctic in pristine and polluted areas (Wiencke and Clayton, 2002). These characteristics rendered *I. cordata* a promising bioindicator for the study of metal levels in seawater and, thus, of the impact of anthropogenic pollution (Dalla Riva et al., 2004). We hypothesize that exposure to elevated lead concentrations (10 μg/L and 50 μg/L) will significantly impact *I. cordata*, focusing on its stress responses and physiological adaptations rather than bioaccumulation. Specifically, we expect to observe reduced photosynthetic apparatus, with potential decreases in phycobiliproteins and compensatory increases in carotenoids. Antioxidant enzyme activities (catalase, ascorbate peroxidase, and superoxide dismutase) are anticipated to rise in response to oxidative stress. We also predict alterations in metabolomic profiles and morphological changes, such as color loss and starch grain variations. These physiological adaptations will help elucidate lead's biochemical impact on *I. cordata* and enhance its use as a bioindicator for future Pb contamination scenarios.

Our study investigates the physiological impact of lead at concentrations higher than those typically reported in Antarctica. While lead levels in Terra Nova Bay during the austral summer of 2011–2012 ranged from 0.4 to 1.0 μg/L (Foltran et al., 1996), the concentrations used in this research align with those found in other regions, such as Casey Station in the Windmill Islands (East Antarctica), where Pb concentrations in *I. cordata* thalli reached up to 21.6 μg g^{-1} (Collén et al., 2003). The chosen lead concentrations were deliberately set higher than current environmental levels to simulate potential future scenarios resulting from climate-induced changes in metal runoff into Antarctic waters (Barbante et al., 1998). By analyzing the effects of lead on photosynthetic pigments, antioxidant enzyme activities, metabolomic profiles, thalli morphology, and cell ultrastructure, we aim to improve the understanding of lead-induced stress responses in *I. cordata*, without focusing on bioaccumulation, but instead emphasizing physiological responses to contamination.

2. Materials and methods

2.1. Experimental setup

I. cordata thalli were collected by scuba divers in November 2021 during the XXXVII Italian Antarctic Expedition at a depth of ~5 m from Punta Stocchino (74°42′ S, 167°7′ E) in Terra Nova Bay (Ross Sea, Antarctica). After sampling, thalli were maintained in thermostatic aquariums in PVC (polyvinyl chloride) filled with oxygenated natural seawater collected from a depth of 5 m (pH 8.03 ± 0.01, oxygen 6.82 ± 0.04 mL/L and salinity 34.79 ± 0.01 PSU) at a temperature of approximately −1 °C in the dark at the Italian Antarctic Station Mario Zucchelli for the acclimation to experimental conditions. To evaluate the effects of lead [lead (II) chloride, Sigma-Aldrich, Auckland, New Zealand] on *I. cordata*, seaweeds were exposed in triplicate to two different Pb concentrations, namely 10 μg/L (LOW) and 50 μg/L (HIGH). A control group (CTRL) without Pb was included. The nominal concentrations were verified by atomic absorption spectrophotometry (ICP–MS) (PerkinElmer SCIEX, Woodbridge, ON, Canada), every two days and were 9.94 ± 1.46 (LOW) and 51.60 ± 5.18 μg/L (HIGH), respectively. The presence of abnormal concentrations of heavy metals (such as Cu, Pb, Al, Fe) was excluded by chemical analysis (in press). Control and treatment thalli were harvested after 10 days of exposure and immediately frozen with liquid nitrogen for subsequent analyses.

2.2. Photosynthetic pigments

2.2.1. Water-soluble pigment content

I. cordata thalli (~1 g of fresh weight) were ground to fine a powder using a mortar, pestle and liquid nitrogen. Samples were homogenized with 1 mL of phosphate buffer (0.01 M sodium phosphate, pH 7.0, 0.15 M NaCl) in Eppendorf tubes, shaken and centrifugated at 11,000*g* for 4 min (3K15, Sigma Laborzentrifugen GmbH, Germany). The supernatant was recovered, and phycobiliprotein contents, expressed as μg g^{-1} fresh weight (FW), were spectrophotometrically determined using the following equations (Bennett and Bogobad, 1973):

$$PC = [(A_{615} - 0.474\,A_{652})/5.34] \times V/W \quad (1)$$

$$APC = [(A_{652} - 0.208\,A_{615})/5.09] \times V/W \quad (2)$$

$$PE = \{[A_{562} - 2.41 \times (PC) - 0.849 \times (APC)]/9.62\} \times V/W \quad (3)$$

where:

W = sample weight (g of fresh weight)
V = phosphate buffer volume (mL)
A_{562}, A_{615}, A_{652} = absorbance at *x* nm.

2.2.2. Liposoluble pigment content

Samples (~1 g of fresh weight) were ground in a mortar with pestle and liquid nitrogen. Thalli powder was mixed with 90 % acetone (1 mL, *v*/v) and incubated overnight at 4 °C. After incubation, samples were centrifugated at 11,000*g* for 4 min at 4 °C, the supernatants were recovered, and their absorbances (A_x) were measured at 750, 664 and 470 nm using a DU530 Beckman Coulter spectrophotometer (Fullerton, California, USA). Pigment concentrations, expressed as μg g^{-1} fresh weight (FW), were estimated using the following equations (Der Bai et al., 2011):

$$Chl\ a = \{[(11.85 \times A_{664}) - (1.54 \times A_{647}) - (0.08 \times A_{630})]/W\} \times V \quad (1)$$

$$Tot\ car = \{[(7.60 \times A_{480}) - (1.49 \times A_{510})]/W\} \times V \quad (2)$$

where:

W = sample weight (g of fresh weight)
V = 90 % acetone volume (mL)
A_x = (absorbance at *x* nm) − (absorbance at 750 nm).

2.3. Antioxidant enzymes

2.3.1. Preparation of the enzymatic extract

Seaweed samples (0.1 g of fresh weight) were ground with mortar and pestle using liquid nitrogen. The obtained powder was transferred in

an Eppendorf tube with 1 ml of homogenization buffer (Tris–HCl 20 mM pH 7.6, EDTA 1 mM, DTT 1 mM, Sucrose 0.5 M and KCl 0.15 M) and centrifugated at 12,000 rpm for 30 min at 4 °C. The supernatant (enzymatic extract) was recovered and used to measure different enzymatic activities.

2.3.2. Total soluble proteins

Total soluble proteins for each enzymatic extract were measured using the method proposed by Bradford (Bradford, 1976) and adapted to 96-well plates. Briefly, 20 µl of enzymatic extract were mixed with 1 mL of Bradford solution (Bio-Rad Protein Assay). Samples were incubated for 10 min at room temperature (RT), and the absorbance at 595 nm was measured by a microplate reader (Tecan Spark GmbH, Austria). A calibration curve using bovine serum albumin (BSA) was used to calculate protein concentration (µg of protein/mL).

2.3.3. Catalase (CAT)

CAT activity was determined as previously described by Aebi (Aebi, 1984). The reaction was started by mixing 620 µl of potassium phosphate buffer (50 mM, pH 7.0), 350 µl of H_2O_2 (10 mM), and 30 µl of the enzymatic extract. The decrease in absorbance was measured at 240 nm for 1 min and expressed as U/mg protein. One unit of CAT was defined as the amount of enzyme catalysing the scavenging of 1 µmol of H_2O_2/min.

2.3.4. Ascorbate peroxidase (APX)

APX activity was measured according to Nakano and Asada (Nakano and Asada, 1981) with modifications (Janknegt et al., 2009). Briefly, 800 µl potassium phosphate buffer (50 mM, pH 7; 0.1 mM EDTA), were mixed with 50 µl of ascorbic acid (10 mM) and 133 µl extract. This mixture was incubated for 5 min at room temperature. The reaction was started by adding 10 µl of H_2O_2 (20 mM). The rate of ascorbate consumption was measured at 290 nm for a time interval of 3 min. APX activity was expressed as U/mg protein. One unit of APX was defined as the amount of enzyme that break down 1 µmol of ascorbate/min.

2.3.5. Superoxide dismutase (SOD)

SOD activity was determined by using a SOD activity assay kit (Merck KGaA, Darmstadt, Germany) following the guidelines provided by the manufacturer on a 96–well plate. Enzyme activity was expressed as U/mg protein, and one unit of SOD was defined as the amount of sample causing 50 % inhibition under the assay conditions.

2.3.6. Glutathione–S–transferase (GST)

GST activity was determined as described by Habig (Habig et al., 1974). Briefly, 800 µl potassium phosphate buffer (0.1 M, pH 6.5) was mixed with 50 µl of chloro–dinitrobenzene (CDNB) 20 mM and 100 µl of GSH solution 0.1 M and incubated at 37 °C for 30 min. Enzyme extract (50 µl) was added, and the absorbance was recorded at 340 nm for 3 min. GST activity was expressed as nmol/min/mg protein.

2.4. Untargeted metabolomics

Acetone extracts from *I. cordata* (CTRL, LOW, HIGH) were analyzed in triplicates by liquid chromatography high–resolution mass spectrometry (LC–HR–MS) using the protocol reported in Silva et al. (Silva et al., 2022). Xcalibur v4.1 Qual Browser (Thermo Scientific, Waltham, MA, USA) was used to acquire LC–MS data. Positive polarity ".raw" data files were converted to ".mzML" format in centroid mode using Proteowizard (Chambers et al., 2012). Mzmine version 3.2.3 (Schmid et al., 2023) was employed for feature finding, alignment and extraction. Final features were exported as ".mgf" and ".csv" files and analyzed in Global Natural Products Social Molecular Networking (Wang et al., 2016) (GNPS; http://gnps.ucsd.edu, accessed on 8 July 2023) platform for feature–based molecular networking (Nothias et al., 2020). The data was filtered by removing all MS/MS fragment ions within ±17 Da of the precursor *m/z*. MS/MS spectra were window-filtered by choosing only the top 6 fragment ions in the ±50 Da window throughout the spectrum. The precursor ion mass tolerance was set to 0.02 Da, and the MS/MS fragment ion tolerance to 0.02 Da. A molecular network was created where edges were filtered to have a cosine score above 0.7 and >4 matched peaks. Further, edges between two nodes were kept in the network if and only if each node appeared in each other's top 10 most similar nodes. Finally, the maximum size of a molecular family was set to 100, and the lowest-scoring edges were removed from molecular families until the molecular family size was below this threshold. The library spectra were filtered in the same manner as the input data. All matches kept between network spectra and library spectra were required to have a score above 0.8 and at least 4 matched peaks. SIRIUS version 5.8.3 (Dührkop et al., 2019) was used to assign features molecular formulas and predict their structures and chemical classes based on the fragmentation patterns in MS/MS spectra and the MS1 (parent ion) isotope patterns (Böcker et al., 2009). Within the workflow, ZODIAC (Ludwig et al., 2020), CSI:FingerID (Hoffmann et al., 2021), and CANOPUS based on ClassyFire ChemOnt ontology (Djoumbou Feunang et al., 2016; Dührkop et al., 2020) tools were employed. Blank was used for background feature removal. Features annotation was based on four distinct levels (Sumner et al., 2007).

2.5. Ultrastructural analyses

I. cordata thalli were cut into small pieces (about 5 mm^2) and fixed overnight at 4 °C in 2.5 % glutaraldehyde and 4 % of paraformaldehyde buffered with 0.1 M sodium cacodylate (pH 7.4). Samples were washed three times for 10 min with sodium cacodylate buffer (0.1 M pH 7.4) at 4 °C and were post–fixed at 4 °C for 2 h in the dark using 1 % (*v*/v) osmium tetroxide (OSO_4) in the same buffer. In the following step, samples were dehydrated using increasing ethanol concentrations [25 %, 50 %, 75 %, 100 % (v/v)]. Each wash was done 2 times for 10 min. After the last 100 % ethanol wash, 3 washes of 15 min with Propylene Oxide were done. The last step was the embedding in epon resin. Samples were put in a blend 1:1 mix ratio of propylene oxide and epon resin, maintained overnight at room temperature. Afterwards, samples were put in tubes with fresh epon resin for 2 h at 37 °C. Then, epon resin was added again, and the samples were kept at 37 °C overnight and 60 °C for 1 day to reach polymerization. The embedded samples were cut into two types of sections. For light microscopy, thin sections (1 µm thick) were cut with an Ultracut Reichert–Jung ultramicrotome, stained with basic toluidine blue (1 % toluidine blue and 1 % Na tetraborate, 1:1 by volume), washed with distilled water, dried, and observed and photographed under a light microscope Leitz DM IRB (Leica, Wetzlar, Germany). For transmission electron microscopy, ultrathin sections (70–80 nm thick), cut with the same ultramicrotome, were post–stained with uranyl acetate and lead citrate and examined and photographed under a transmission electron microscope FEI Tecnai G2 (FEI, Eindhoven, Netherlands), equipped with a side-mounted camera Olympus Veleta (Olympus, Münster, Germany) and a bottom-mounted camera TVIPS F114 (TVIPS, Gauting, Germany).

2.6. Statistical analysis

Three biological replicates were considered for each concentration treatment group (CTRL, LOW and HIGH). Two technical replicates were conducted for CAT, APX and GST, while three technical replicates were analyzed for SOD. Statistical analyses were performed in R–Statistics 3.2.3 version. The normal distribution (Shapiro–Wilk's Normality Test) and the homogeneity of the variance (Levene's test) were assessed. Pigment and enzymatic assay data were analyzed using one–way ANOVA or its non–parametric equivalent (Kruskal–Wallis test), followed by Turkey's post–hoc or non–parametric post–hoc test (Dunn test). Metabolomics data were analyzed through different steps (multivariate and univariate). After blank removal and data normalization, the "pheatmap" package was employed for heatmap visualization. PCA

visualization was performed based on Euclidean distances to examine sample clustering followed by a PERMANOVA test (n permutation = 999) using "vegan", "RVAideMemoire", "factoextra", "ggforce", and "ggplot2" R packages. Four additional R packages ("ggsci", "matrixStats", "ggrepel", and "tidyverse") were used to compare treatment and control samples by one–way ANOVA followed by Tukey's post hoc test.

3. Results

3.1. Photosynthetic pigments

Phycobiliprotein, chlorophyll *a* (Chl *a*) and total carotenoid contents (Fig. 1, Tables S1–5) were measured after ten days of exposure to lead. Phycocyanin (PC) and phycoerythrin (PE) significantly decreased in the thalli exposed to lead (Fig. 1a, b), while no statistically significant differences were observed for allophycocyanin (APC) (Fig. 1c) and for chlorophyll *a* (Chl *a*) content (Fig. 1d). *I. cordata* thalli showed an increase in the total amount of carotenoids (Fig. 1e). This increase was not statistically significant in thalli exposed at 10 µg/L (LOW) of lead (p–values > 0.05), while it was significant (p–values < 0.05) in those exposed at 50 µg/L (HIGH) of Pb (Table S5).

3.2. Antioxidant enzymes

Antioxidant enzyme activities (Fig. 2) were determined for CAT, APX, SOD and GST. CAT activity in the thalli of *I. cordata* was affected only by a high lead concentration (Fig. 2a), with a significant increase in CAT activity between CTRL and HIGH (Table S6). Statistical analysis showed significant differences in the APX activity (Fig. 2b) between HIGH and LOW treatments and between HIGH and CTRL samples. In contrast, no statistical differences were observed among CTRL and LOW thalli (Table S7). SOD activity increased after lead exposition in both

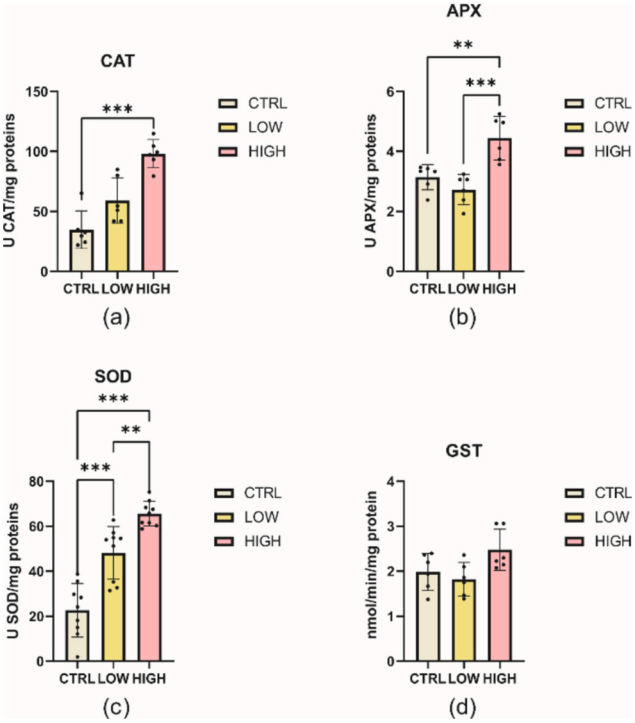

Fig. 2. Variations on CAT (a), APX (b), SOD (c) and GST (d) activities in thalli of *I. cordata* exposed to different concentrations of lead CTRL (ivory), LOW (yellow) and HIGH (pink). Results are expressed as mean ± standard deviation. Asterisks indicate statistically significant differences ('***' = p–value < 0.001; '**' = p–value < 0.01 and '*' = p–value < 0.05).

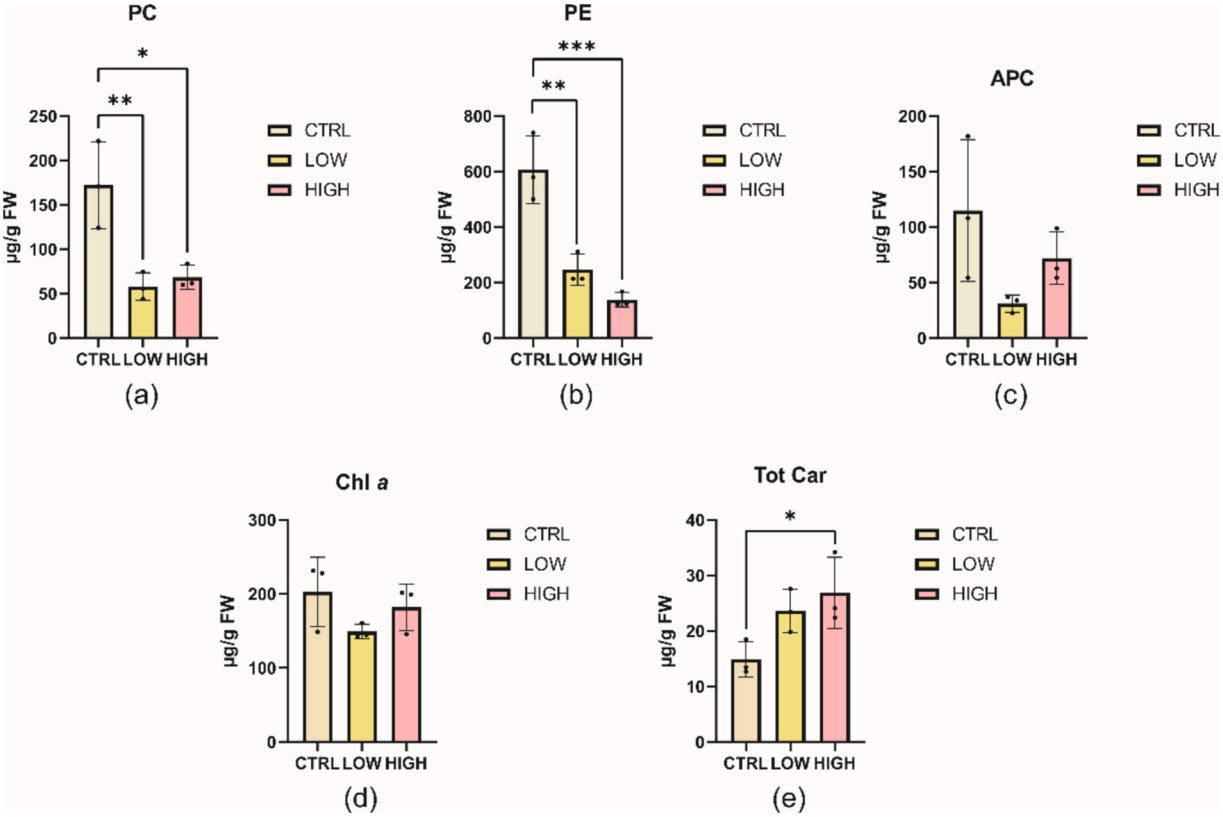

Fig. 1. Phycocyanin (PC), phycoerythrin (PE), allophycocyanin (APC), chlorophyll *a* (Chl *a*) and total carotenoid (Car tot) content of *I. cordata* exposed to different concentrations of lead CTRL (ivory), LOW (yellow) and HIGH (pink). Results are expressed as mean ± standard deviation. Asterisks indicate statistically significant differences ('***' = p–value < 0.001; '**' = p–value < 0.01 and '*' = p–value < 0.05).

LOW and HIGH treatments compared to the control (Fig. 2c). In contrast to CAT and APX, the activity of SOD was significantly affected by lead exposure not only at high concentrations but also at lower concentrations (Table S8). GST activity was constant in *I. cordata* lead treatments and controls (Fig. 2d), and no statistical differences were reported (Table S9).

3.3. Untargeted metabolomics

The metabolomic profiles of *I. cordata* acetone extracts recovered from control and lead-treated samples were determined through an untargeted UPLC–HR–MS/MS approach in triplicates. A principal component analysis (PCA) based on *I. cordata* metabolomes (Fig. 3) highlighted treatment–related clustering of the biological replicates. The 71.3 % of the variance among replicates was accounted by the first component (PC 1) separating CTRL samples from LOW and HIGH treatments. The second component (PC 2) accounted for 9.8 % of the variance and did not allow a clear clustering of the replicates. Overall, PCA evidenced distinct metabolic signatures after lead exposure, as shown in PERMANOVA analysis (Table S10).

Out of the 291 features obtained in this experiment (Table S11), 192 features (66 % of the total) were not significantly different between control and lead–treated samples (p–value > 0.05), while 99 features (34 % of the total) displayed significant (p–value < 0.05) differences (Fig. S1). As for the whole metabolome, a PERMANOVA was performed to identify variations in major chemical classes after lead exposure (Table S10). Statistical differences were reported for fatty acyls, the main class of compounds recovered in this study. In contrast, no significant differences were reported for glycerolipids and glycerophospholipids, organonitrogen, organooxygen compounds, and tetrapyrroles. Each feature was compared among different treatments using Tukey's post hoc test (Tables S12–S14), and the results of statistical analyses were visualized using volcano plots (Figs. S2–S4). Features extracted in this study were visualized singularly, using boxplots (Fig. S5), and collectively through a hierarchical clustering heatmap (Fig. 4), including annotated compound classes.

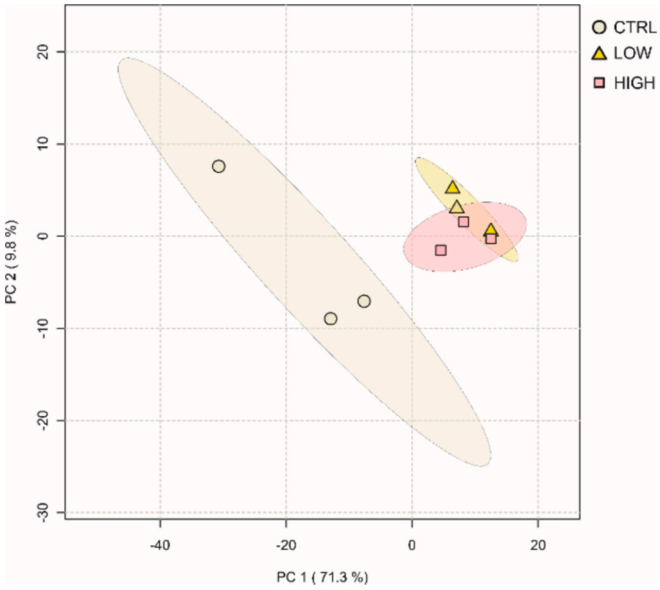

Fig. 3. Principal component analysis (PCA) of metabolomic profiles of *I. cordata* after led exposure. The x– and y–axes represent principal component 1 and 2, respectively, in brackets the percentages of the overall variance explained by each principal coordinate. PERMANOVA analysis proved distinct metabolomes at different temperatures (p–value < 0.05). Ivory circles, CTRL; yellow triangles, LOW; pink squares, HIGH.

3.4. Morphological and ultrastructural analyses

Control lamina of *I. cordata* presented the typical reddish color and the characteristic iridescence accounting for the name of the genus *Iridaea* (Foltran et al., 1996), while thalli exposed to lead showed a reduction in the reddish coloration (Fig. 5). Through scanning electron microscope observations, *I. cordata* cells exhibited chloroplasts with a single peripheral thylakoid surrounding internal unstacked thylakoidal membranes, irregular cytoplasmic profiles and cell walls consisting of parallel microfibrils encircling the cells (Fig. 6a–f). At a low lead concentration (10 μg/L), chloroplast displayed an increased number of plastoglobuli compared to controls (Fig. 6c, d). *I. cordata* cells of thalli exposed to high lead concentration (50 μg/L) numerous large plastoglobuli (Fig. 6e) and large floridean starch granules located near the pit connections (Fig. 6f).

4. Discussion

4.1. Photosynthetic pigments

Alterations in photosynthetic pigments are frequently used to assess metal stress in algae (Chu et al., 2019; Ralph et al., 2007). Thus, in this study, we evaluated phycobiliproteins, Chl *a* and total carotenoid content after the exposure of *I. cordata* at 10 μg/L and 50 μg/L of lead. Our results highlighted a significant decrease of two phycobiliproteins extracted from *I. cordata*, namely phycocyanin and phycoerythrin, among control and treatments. Similar results were obtained in other Rhodophyta, such as *Gelidium floridanum* exposed at 10 and 20 mg/L of lead (dos Santos et al., 2014), *Gracilaria domingensis* exposed to 5 and 10 mg/L of lead (Gouveia et al., 2013) and *G. domingensis* exposed to 20 mg/L, 40 mg/L and 60 mg/L of cadmium (dos Santos et al., 2014). The decrease of PE and PC contents might be related to phycobilisome damages, a typical response of red seaweeds underlying metal stress (Zhu et al., 2017; Xia et al., 2004). Chl *a* concentration did not show statistically significant differences between controls and treatments in *I. cordata*, suggesting that lead exposure did not affect this pigment. Comparable findings were previously reported in red seaweed of *G. dominigensis* exposed to 5 mg/L of lead and to 5 mg/L of copper (Gouveia et al., 2013), and in *Gracilaria lemaneiformis* after copper exposure at 0.5, 1.0 and 2.0 mg/L (Xia et al., 2004). On the other hand, several studies on Rhodophyta reported a significant decrease in chlorophyll due to metal exposure. A reduction in Chl *a* was highlighted in *Sarcodia suiae* exposed to 5 mg/L of lead (Chang et al., 2023b), *G. dominigensis* exposed to 5 mg/L of copper (Gouveia et al., 2013) and *Pseudokirchneriella subcapitata* exposed to 2 mg/L of cadmium (Gouveia et al., 2013) and 1 mg/L of copper (Machado et al., 2015). An increase in total carotenoids was observed in *I. cordata* exposed to lead, and there was a significant difference between CTRL and HIGH samples. Carotenoids are known as lipophilic antioxidants synthesized and stored in seaweed chloroplasts, protecting cells from free radicals (Rezayian et al., 2019). The production of carotenoids is a common strategy in Rhodophyta to prevent the harmful effects of ROS and metals, as demonstrated in *G. domingensis* (Gouveia et al., 2013) exposed to a lead concentration of 5 mg/L and *Gelidium floridanum* (dos Santos et al., 2014) exposed to 10 and 20 mg/L of lead. The results obtained in *I. cordata* corroborate previous evidence on the effects of metals on algae, indicating that changes in photosynthetic pigment content are species– and stress–-specific and strongly dependent on metal concentration and exposure time (Mallick and Mohn, 2000; Chakraborty et al., 2014).

4.2. Antioxidant enzymes

The toxic effects of lead and other metals are also related to ROS production, resulting in unbalanced cellular redox status (Pinto et al., 2003). Different antioxidant enzymatic activities were measured to investigate the effects of lead exposure in *I. cordata*. The present study

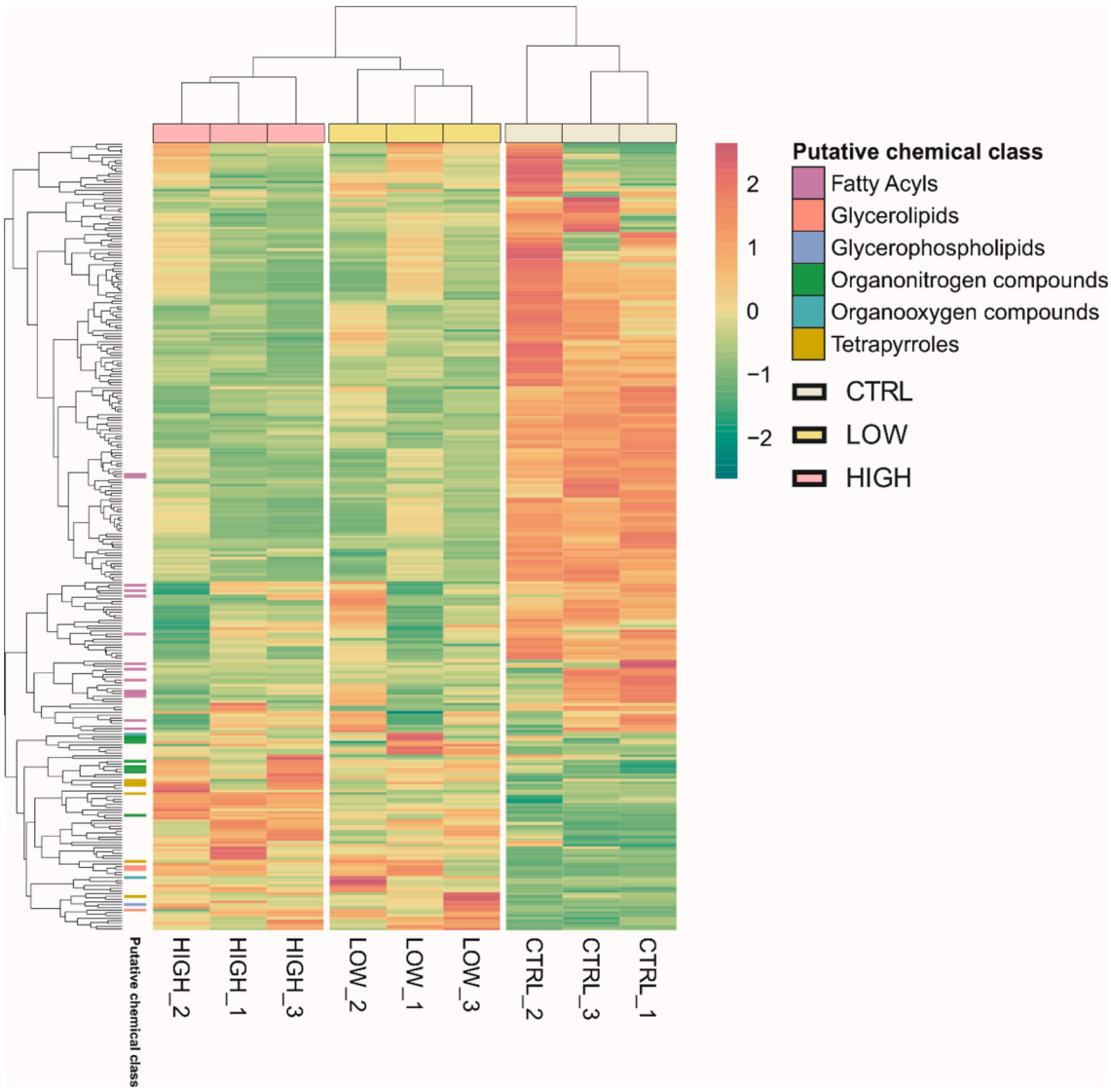

Fig. 4. Hierarchical clustering analysis of *I. cordata* metabolomes after lead exposure. Colors from blue to red indicate the normalized relative abundance of metabolites from low to high according to the scale bar. Samples of *I. cordata* exposed to different lead concentrations CTRL (ivory), LOW (yellow) and HIGH (pink) are reported in columns; replicates are indicated with the treatment condition (CTRL, LOW, HIGH) followed by the suffix number (1, 2 and 3). Feature chemical classes are shown in different colors.

Fig. 5. Imagines of CTRL (a), LOW (b) and HIGH (c) thalli of *I. cordata*. Scale bar: (a, b, c) = 1 cm.

observed a significant increase in CAT activity in samples exposed at 50 μg/L of Pb, while no significant differences were reported among controls and samples treated with 10 μg/L of Pb. The increase in CAT activity at higher Pb concentration confirmed previous reports on other species of Rhodophyta, such as *Gracilaria tenuistipitata* exposed at 200 μg/L of Cu and 100 μg/L of Cd (Collén et al., 2003), and *Gracilaria manilaensis* exposed at 2 mg/L of Pb (Ahamad and Shuhanija, 2013). CAT activity increases with the increase of lead concentration, thus with ROS production deriving from metal intake (Pinto et al., 2003), and is a typical response to metal stress in seaweeds (Collén et al., 2003; Ahamad and Shuhanija, 2013). A significant increase in APX activity was measured among *I. cordata* control thalli and those treated with 50 μg/L

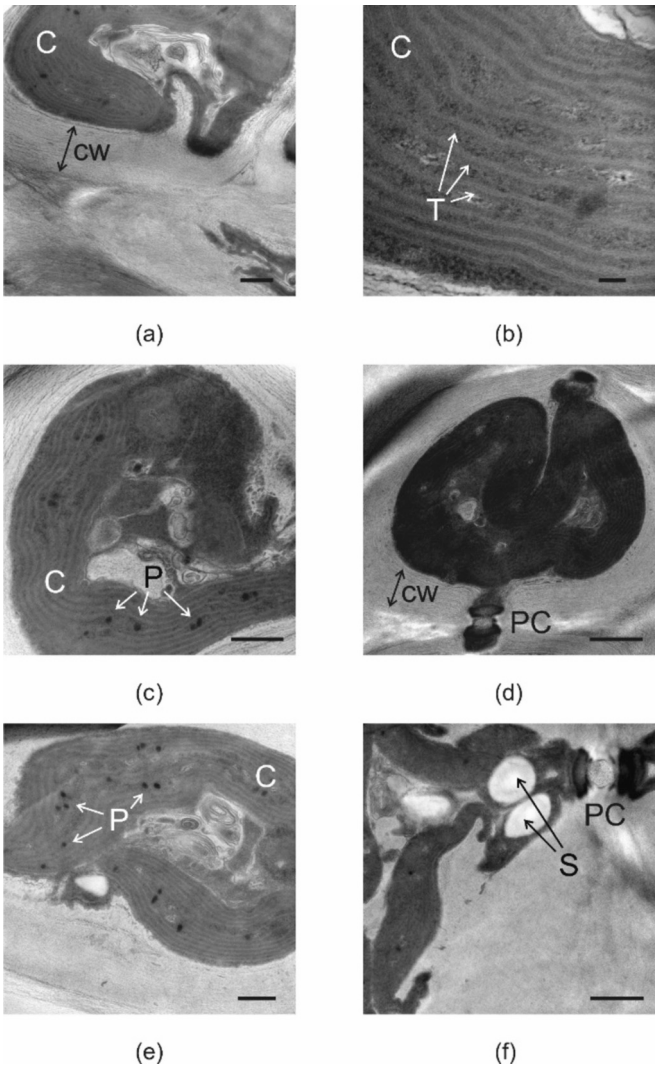

Fig. 6. Transmission electron microscope images CTRL (a, b), LOW (c, d) and HIGH (e, f) cells of *I. cordata*. Chloroplast I; cell wall (CW); thylakoidal membranes (T); plastoglobuli (P); pit connections (PC); starch granules (S). Scale bar: (a, c, e) = 500 nm; (b) = 100 nm; (d, f) = 1 μm.

of Pb. These results likely represent a response to metal–related oxidative stress, using ascorbate as a hydrogen donor to scavenge H_2O_2 and producing H_2O and monodehydroascorbate (Gouveia et al., 2013; Ahamad and Shuhanija, 2013). Our findings corroborated similar observations reported in red seaweeds, such as *Gracilaria manilaensis* exposed at 2 mg/L of lead (Ahamad and Shuhanija, 2013), and other algae, such as *Chlorella sorokiniana* and *Scenedesmus acuminatus* exposed at 1.5 mg/L and 3 mg/L of copper (Hamed et al., 2017). SOD, which the dismutation of $^{\bullet}O_2^{\bullet-}$ to O_2 and H_2O_2, is considered as the cell's first line of defense against ROS (Pinto et al., 2003; Ferro et al., 2013; Chatzidimitriou et al., 2020; Schumann et al., 2023). $^{\bullet}O_2^{\bullet-}$ is a precursor of other highly reactive species. Thus, SOD activity prevents the further generation of free radicals (Pinto et al., 2003; Mallick and Mohn, 2000). Our results highlighted a significant increase of SOD activity in the thalli exposed to both 10 μg/L and 50 μg/L of Pb. The pronounced increase in SOD activity, even at low lead concentrations, suggests that this enzyme represents an important defense against lead and other metal–related oxidant stress in *I. cordata*, as reported for the red alga *Gracilaria tenuistipitata* exposed to 0.2 mg/L of copper and 1 mg/L of cadmium (Collén et al., 2003). The early and significant induction of SOD activity, even at low Pb concentration in our study, suggests its pivotal role as the first line of defense against ROS, preventing the accumulation of superoxide radicals and subsequent oxidative damage. Overall, our results suggest an initial increase in $^{\bullet}O_2^{\bullet-}$ production resulting in the induction of SOD. The H_2O_2 produced by this enzyme is subsequently eliminated by CAT and APX, mitigating its toxic effect primarily at higher lead concentrations. At lower concentrations, other enzymes are likely to intervene that are known to act effectively in scavenging H_2O_2 and other peroxides, such as glutathione peroxidases and peroxiredoxins (Santovito et al., 2012; Pacchini et al., 2023; Tolomeo et al., 2016). Thus, these two enzymes might act as complementary defense mechanisms in response to lead. Finally, GST activity was measured to investigate the effects of lead exposure on *I. cordata*. GST belongs to a family of isoenzymes known for their capacity to catalyze the conjugation of the reduced form of glutathione (GSH) to xenobiotic substrate to allow ROS detoxification. The resulting conjugates are water soluble and easily excretable (Maharana et al., 2010). Although GST is not considered an antioxidant enzyme, it plays a crucial role in the antioxidant defense system of cells by indirectly maintaining redox balance (de Obeso Fernández et al., 2023). However, while an increase in this enzyme activity was reported in the green algae *Scenedesmus obliquus* (Dewez et al., 2005) exposed at 3 mg/L of copper, our results did not show statistically significant differences among treatments and control. This might be likely due to the low lead concentration considered in our experiment. Further studies should investigate the involvement of different enzymes to elucidate the complex dynamics of antioxidant defense mechanisms under varying metal stress conditions.

4.3. Untargeted metabolomics

Untargeted metabolomics, employing liquid chromatography (LC) with high-resolution tandem mass spectrometry (MS/MS), was used to investigate biochemical differences between control and lead–treated thalli of *I. cordata*. Our results highlighted distinct clustering of *I. cordata* metabolomes, as shown in the PCA plot and supported by PERMANOVA analysis. Combining mass spectral libraries matches with in–silico tools for feature annotation enabled the association of 11.7 % of the detected features to a chemical class. Following this approach, we found chemical characteristics of metabolites that differentiate *I. cordata* metabolomes after lead exposure. Fatty acyls were the only chemical class showing statistically significant variation in *I. cordata* metabolome. Fatty acyls are an essential category of lipids involved in a wide range of biological functions, including several subclasses (De Luca et al., 2021). Algal lipids, particularly polyunsaturated fatty acids constituting chloroplast membranes, are direct targets for peroxidation due to the presence of metal–induced ROS (Rezayian et al., 2019). In addition, xenobiotics, including metals, can interfere with fatty acids synthesis, thus affecting fatty acids composition and productivity (Filimonova et al., 2016; Andrade et al., 2021). Together with changes in lipids, Pb is known to strongly inhibit enzymes involved in chlorophyll biosynthesis and the Calvin cycle, leading to a decrease in the photosynthetic rate (Nowicka, 2022). No significant differences were detected in tetrapyrroles, a class of molecules, such as chlorophylls, able to absorb visible light (Brzezowski et al., 1847), in *I. cordata*. However, the results of the PERMANOVA analysis showed a relatively low p–value (p–value $<$ 0.10), indicating a possible effect of lead in chlorophyll and its catabolites. When features annotated as tetrapyrroles were considered separately, a significant increase in pheophorbide *a* (Feature ID: 681), a product of Chl *a* degradation (Schelbert et al., 2009), was reported in *I. cordata* samples exposed to 50 μg/L of Pb. No significant differences were reported among CTRL, LOW and HIGH samples for pheophytin *a* (Feature ID: 660), another Chl *a* catabolite, as well as other features annotated as tetrapyrroles (Feature ID: 725, 729, 738 and 820). These results confirmed those highlighted in the spectrophotometric quantification of Chl *a* and suggested that Pb concentrations employed in this study were too low to affect chlorophyll and its derivatives. Finally, metabolic features were through hierarchical cluster analysis and listed in supplementary material, thus providing a catalogue of possible

biomarkers that can be targeted in future studies on the response of Rhodophyta to lead exposure.

4.4. Morphological and ultrastructural analyses

The loss of reddish color observed in samples treated with lead is likely due to the decrease of phycobiliproteins (PC and PE), as previously reported in the red seaweed *G. floridanum* after exposure to Pb and other metals like Cd and Cu (dos Santos et al., 2014). Dos Santos et al. speculated that the decrease in phycobiliproteins in Rhodophyta treated with metals might be a mechanism to prevent the excess of excitation energy in the chloroplasts, thus avoiding a further increase in ROS levels (dos Santos et al., 2014). Our results supported this hypothesis. Nevertheless, future studies on metal interaction with phycobilisomes and phycobiliproteins are required. Transmission electron microscopy (TEM) highlighted ultrastructural differences in *I. cordata* cells among control and treatments. CTRL cells presented chloroplasts with the typical internal organization of the red algae (Pueschel, 1990), consisting of a single peripheral encircling thylakoid and a variable number of evenly spaced thylakoids (Navarro et al., 2010). Lead–treated cells showed an increase in the number of plastoglobuli, electron–dense lipid droplets with a reserve role (Schmidt et al., 2009), between the thylakoids. A similar increase in plastoglobuli was observed in several species of red macroalgae exposed to metals, such as *Ceramium ciliatum* exposed to Zn and Cd (Diannelidis and Delivopoulos, 1997), *G. domingensis* treated with Cd (dos Santos et al., 2013), *Geldum floridanum* exposed to Cd, Cu and Pb (dos Santos et al., 2014) and *Pterocladiella capillacea* subjected to Cd treatment (Marthiellen et al., 2014). The increase in the number of plastoglobuli, thus an accumulation of lipids, is a common response to metal stress in red seaweeds, which dos Santos et al. interpreted as a change in lipid metabolism (dos Santos et al., 2012). These results are based on the variations in fatty acyls in the *I. cordata* metabolome, as reported in the previous section. Future studies targeting the effects of lead on lipid metabolism in Rhodophyta are required to better understand the biochemical implications of leads and other metals on these marine phototrophs. Floridean starch grains located near pit connections were observed in cells of *I. cordata* treated with 50 μg/L of Pb. While an increase in the number of floridean starch grains was found in *Gracilaria domingensis* (dos Santos et al., 2013) treated with Cd, a decrease in starch grains was reported for *H. musciformis* after treatment Cd (Bouzon et al., 2012). A copper–induced reduction in the synthesis of floridean starch grains was reported for *G. domingensis* (Gouveia et al., 2013). These findings suggest possible metal– and species–specific mechanisms resulting from metal exposure.

5. Conclusions

This study aimed to understand the effects of environmental concentrations of lead in the red alga *I. cordata* as a proxy for future investigations of metal contamination in Antarctica and its possible effects on marine life. The results obtained in this study showed alterations in photosynthetic pigments, particularly in phycocyanin, phycoerythrin and total carotenoids, as a response to Pb. The enzymatic analyses showed a significant increase in activities CAT, APX and SOD suggesting an efficient antioxidant response of *I. cordata* to Pb concentrations employed in this study. Untargeted metabolomics was used as a preliminary tool to investigate the biochemical effect of Pb in *I. cordata* metabolism. Our results highlighted that fatty acyls were the only chemical class significantly affected by lead, thus indicating molecules belonging to this group as possible biomarkers in studying metal–induced stress. Morphological analyses of the thalli showed the loss of reddish color in samples after Pb exposure, corroborating the results of pigment analysis. Observations of *I. cordata* cell ultrastructure highlighted an accumulation of floridean starch grains and an increase in electron–dense lipid droplets, known as plastoglobuli, suggesting a change in lipid metabolism, as highlighted in the study of *I. cordata* metabolome. Further data are necessary to clarify the effects of different lead concentrations and other metals on Antarctic Rhodophyta, which is mandatory in the context of conservation and local marine biodiversity. Given the unique nature of Antarctica, the ecological relevance of these findings is significant. *I. cordata* has demonstrated potential as a bioindicator species, capable of reflecting early signs of metal contamination in polar marine ecosystems. By identifying key physiological and metabolic responses, this study provides foundational knowledge for using *I. cordata* as an indicator species in conservation efforts aimed at preserving Antarctic marine biodiversity.

Supplementary data to this article can be found online at https://doi.org/10.1016/j.cbpc.2024.110063.

Funding

This research was supported by the Italian National Program for Antarctic Research (PNRA) [project code: 2018/B2Z1.01]; the Portuguese national funds from FCT—Foundation for Science and Technology [projects UIDB/04326/2020 (DOI:10.54499/UIDB/04326/2020), UIDP/04326/2020 (DOI:10.54499/UIDP/04326/2020), and LA/P/0101/2020 (DOI:10.54499/LA/P/0101/2020]. Luísa Custódio was supported by the FCT Scientific Employment Stimulus (CEEC-IND/00425/2017).

CRediT authorship contribution statement

Riccardo Trentin: Writing – original draft, Visualization, Validation, Software, Methodology, Investigation, Formal analysis, Data curation, Conceptualization. **Ilaria Nai:** Investigation, Formal analysis, Data curation. **Sophia Schumann:** Writing – review & editing, Investigation, Formal analysis, Data curation. **Gianfranco Santovito:** Writing – original draft, Validation, Supervision, Resources, Funding acquisition, Conceptualization. **Emanuela Moschin:** Writing – review & editing, Validation, Investigation, Formal analysis, Data curation. **Luísa Custódio:** Writing – review & editing, Validation, Supervision, Resources, Methodology, Funding acquisition. **Isabella Moro:** Writing – review & editing, Validation, Supervision, Resources, Funding acquisition, Conceptualization.

Declaration of competing interest

The authors declare that they have no known competing financial interests or personal relationships that could have appeared to influence the work reported in this paper.

Acknowledgments

We wish to thank Dr. José Paulo da Silva (Centre of Marine Sciences, Faculty of Sciences and Technology, University of Algarve, Ed. 7, Campus of Gambelas, 8005–139 Faro, Portugal) for his assistance with the LC–MS analyses.

Data availability

Data will be made available on request.

References

Aebi, H., 1984. [13] Catalase in vitro. Methods Enzymol. 105, 121–126. https://doi.org/10.1016/S0076-6879(84)05016-3.

Ahamad, Z.H., Shuhanija, S.N., 2013. Physiological and biochemical responses of a Malaysian red alga, *Gracilaria manilaensis*, treated with copper, lead, and mercury. J. Environ. Res. Dev. 7, 1246–1253.

Andrade, L.M., Tito, C.A., Mascarenhas, C., Lima, F.A., Dias, M., Andrade, C.J., Mendes, M.A., Nascimento, C.A.O., 2021. *Chlorella vulgaris* phycoremediation at low Cu+2 contents: proteomic profiling of microalgal metabolism related to fatty acids and CO2 fixation. Chemosphere 284, 131272. https://doi.org/10.1016/J.CHEMOSPHERE.2021.131272.

Barbante, C., Turetta, C., Gambaro, A., Capodaglio, G., Scarponi, G., 1998. Sources and origins of aerosols reaching Antarctica as revealed by lead concentration profiles in shallow snow. Ann. Glaciol. 27, 674–678. https://doi.org/10.3189/1998aog27-1-674-678.

Bargagli, R., 2008. Environmental contamination in Antarctic ecosystems. Sci. Total Environ. 400, 212–226. https://doi.org/10.1016/j.scitotenv.2008.06.062.

Bennett, A., Bogobad, L., 1973. Complementary chromatic adaptation in a filamentous blue-green alga. J. Cell Biol. 58, 419–435. https://doi.org/10.1083/jcb.58.2.419.

Böcker, S., Letzel, M.C., Lipták, Z., Pervukhin, A., 2009. SIRIUS: decomposing isotope patterns for metabolite identification. Bioinformatics 25, 218–224. https://doi.org/10.1093/BIOINFORMATICS/BTN603.

Bouzon, Z.L., Ferreira, E.C., dos Santos, R., Scherner, F., Horta, P.A., Maraschin, M., Schmidt, É.C., 2012. Influences of cadmium on fine structure and metabolism of *Hypnea musciformis* (Rhodophyta, Gigartinales) cultivated in vitro. Protoplasma 249, 637–650. https://doi.org/10.1007/S00709-011-0301-6.

Bradford, M.M., 1976. A rapid and sensitive method for the quantitation of microgram quantities of protein utilizing the principle of protein-dye binding. Anal. Biochem. 72, 248–254. https://doi.org/10.1016/0003-2697(76)90527-3.

Brzezowski, P., Richter, A.S., Grimm, B., 1847. Regulation and function of tetrapyrrole biosynthesis in plants and algae. Biochim. Biophys. Acta Bioenerg. 2015, 968–985. https://doi.org/10.1016/J.BBABIO.2015.05.007.

Chakraborty, S., Bhattacharya, T., Singh, G., Maity, J.P., 2014. Benthic macroalgae as biological indicators of heavy metal pollution in marine environments: a biomonitoring approach for pollution assessment. Ecotoxicol. Environ. Saf. 100, 61–68. https://doi.org/10.1016/J.ECOENV.2013.12.003.

Chambers, M.C., MacLean, B., Burke, R., Amodei, D., Ruderman, D.L., Neumann, S., Gatto, L., Fischer, B., Pratt, B., Egertson, J., Hoff, K., Kessner, D., Tasman, N., Shulman, N., Frewen, B., Baker, T.A., Brusniak, M.Y., Paulse, C., Creasy, D., Flashner, L., Kani, K., Moulding, C., Seymour, S.L., Nuwaysir, L.M., Lefebvre, B., Kuhlmann, F., Roark, J., Rainer, P., Detlev, S., Hemenway, T., Huhmer, A., Langridge, J., Connolly, B., Chadick, T., Holly, K., Eckels, J., Deutsch, E.W., Moritz, R.L., Katz, J.E., Agus, D.B., MacCoss, M., Tabb, D.L., Mallick, P., 2012. A cross-platform toolkit for mass spectrometry and proteomics. Nat. Biotechnol. 30, 918–920. https://doi.org/10.1038/nbt.2377.

Chang, C.C., Tseng, C.C., Han, T.W., Barus, B.S., Chuech, J.Y., Cheng, S.Y., 2023a. Effects of lead and zinc exposure on uptake and exudation levels, chlorophyll-a, and phycobiliproteins in *Sarcodia suiae*. Int. J. Environ. Res. Public Health 20, 2821. https://doi.org/10.3390/ijerph20042821.

Chang, C.C., Tseng, C.C., Han, T.W., Barus, B.S., Chuech, J.Y., Cheng, S.Y., 2023b. Effects of lead and zinc exposure on uptake and exudation levels, chlorophyll-a, and phycobiliproteins in *Sarcodia suiae*. Int. J. Environ. Res. Public Health 20, 2821. https://doi.org/10.3390/IJERPH20042821.

Chatzidimitriou, E., Bisaccia, P., Corrà, F., Bonato, M., Irato, P., Manuto, L., Toppo, S., Bakiu, R., Santovito, G., 2020. Copper/zinc superoxide dismutase from the crocodile icefish *Chionodraco hamatus*: antioxidant defense at constant sub-zero temperature. Antioxidants 9, 325. https://doi.org/10.3390/ANTIOX9040325.

Chu, W.L., Dang, N.L., Kok, Y.Y., Ivan Yap, K.S., Phang, S.M., Convey, P., 2019. Heavy metal pollution in Antarctica and its potential impacts on algae. Polar Sci. 20, 75–83. https://doi.org/10.1016/j.polar.2018.10.004.

Collén, J., Pinto, E., Pedersén, M., Colepicolo, P., 2003. Induction of oxidative stress in the red macroalga *Gracilaria tenuistipitata* by pollutant metals. Arch. Environ. Contam. Toxicol. 45, 337–342. https://doi.org/10.1007/s00244-003-0196-0.

Dalla Riva, S., Abelmoschi, M.L., Magi, E., Soggia, F., 2004. The utilization of the Antarctic environmental specimen bank (BCAA) in monitoring Cd and Hg in an Antarctic coastal area in Terra Nova Bay (Ross Sea—Northern Victoria Land). Chemosphere 56, 59–69. https://doi.org/10.1016/j.chemosphere.2003.12.026.

De Luca, M., Pappalardo, I., Limongi, A.R., Viviano, E., Radice, R.P., Todisco, S., Martelli, G., Infantino, V., Vassallo, A., 2021. Lipids from microalgae for cosmetic applications. Cosmetics 8, 52. https://doi.org/10.3390/COSMETICS8020052.

de Obeso Fernández, A., del Valle, C.Q., Scheckhuber, D.A., Chavaro-Pérez, E., Ortega-Barragán, S.K., 2023. Maciver, mRNA sequencing reveals upregulation of glutathione S-transferase genes during *Acanthamoeba* encystation. Microorganisms 11, 992. https://doi.org/10.3390/MICROORGANISMS11040992.

Der Bai, M., Cheng, C.H., Wan, H.M., Lin, Y.H., 2011. Microalgal pigments potential as byproducts in lipid production. J. Taiwan Inst. Chem. Eng. 42, 783–786. https://doi.org/10.1016/j.jtice.2011.02.003.

Dewez, D., Geoffroy, L., Vernet, G., Popovic, R., 2005. Determination of photosynthetic and enzymatic biomarkers sensitivity used to evaluate toxic effects of copper and fludioxonil in alga *Scenedesmus obliquus*. Aquat. Toxicol. 74, 150–159. https://doi.org/10.1016/J.AQUATOX.2005.05.007.

Diannelidis, B.E., Delivopoulos, S.G., 1997. The effects of zinc, copper and cadmium on the fine structure of *Ceramium ciliatum* (Rhodophyceae, Ceramiales). Mar. Environ. Res. 44, 127–134. https://doi.org/10.1016/S0141-1136(96)00106-7.

Djoumbou Feunang, Y., Eisner, R., Knox, C., Chepelev, L., Hastings, J., Owen, G., Fahy, E., Steinbeck, C., Subramanian, S., Bolton, E., Greiner, R., Wishart, D.S., 2016. ClassyFire: automated chemical classification with a comprehensive, computable taxonomy. J. Chem. 8, 1–20. https://doi.org/10.1186/S13321-016-0174-Y.

dos Santos, R.W., Schmidt, É.C., Martins, R. de P., Latini, A., Maraschin, M., Horta, P.A., Bouzon, Z.L., 2012. Effects of cadmium on growth, photosynthetic pigments, photosynthetic performance, biochemical parameters and structure of chloroplasts in the agarophyte *Gracilaria domingensis* (Rhodophyta, Gracilariales). Am. J. Plant Sci. 3, 1077–1084. https://doi.org/10.4236/AJPS.2012.38129.

dos Santos, R.W., Schmidt, É.C., Bouzon, Z.L., 2013. Changes in ultrastructure and cytochemistry of the agarophyte *Gracilaria domingensis* (Rhodophyta, Gracilariales) treated with cadmium. Protoplasma 250, 297–305. https://doi.org/10.1007/S00709-012-0412-8/FIGURES/9.

dos Santos, R.W., Schmidt, É.C., Felix, M.R. de L., Polo, L.K., Kreusch, M., Pereira, D.T., Costa, G.B., Simioni, C., Chow, F., Ramlov, F., Maraschin, M., Bouzon, Z.L., 2014. Bioabsorption of cadmium, copper and lead by the red macroalga Gelidium floridanum: physiological responses and ultrastructure features. Ecotoxicol. Environ. Saf. 105, 80–89. https://doi.org/10.1016/J.ECOENV.2014.02.021.

Dührkop, K., Fleischauer, M., Ludwig, M., Aksenov, A.A., Melnik, A.V., Meusel, M., Dorrestein, P.C., Rousu, J., Böcker, S., 2019. SIRIUS 4: a rapid tool for turning tandem mass spectra into metabolite structure information. Nat. Methods 16, 299–302. https://doi.org/10.1038/s41592-019-0344-8.

Dührkop, K., Nothias, L.F., Fleischauer, M., Reher, R., Ludwig, M., Hoffmann, M.A., Petras, D., Gerwick, W.H., Rousu, J., Dorrestein, P.C., Böcker, S., 2020. Systematic classification of unknown metabolites using high-resolution fragmentation mass spectra. Nat. Biotechnol. 39, 462–471. https://doi.org/10.1038/s41587-020-0740-8.

Ferro, D., Franchi, N., Mangano, V., Bakiu, R., Cammarata, M., Parrinello, N., Santovito, G., Ballarin, L., 2013. Characterization and metal-induced gene transcription of two new copper zinc superoxide dismutases in the solitary ascidian *Ciona intestinalis*. Aquat. Toxicol. 140–141, 369–379. https://doi.org/10.1016/J.AQUATOX.2013.06.020.

Filimonova, V., Gonçalves, F., Marques, J.C., De Troch, M., Gonçalves, A.M.M., 2016. Fatty acid profiling as bioindicator of chemical stress in marine organisms: a review. Ecol. Indic. 67, 657–672. https://doi.org/10.1016/J.ECOLIND.2016.03.044.

Foltran, A., Maranzana, G., Rascio, N., Scarabel, L., Talarico, L., Andreoli, C., 1996. *Iridaea cordata* from Antarctica: an ultrastructural, cytochemical and pigment study. Bot. Mar. 39, 533–541. https://doi.org/10.1515/botm.1996.39.1-6.533.

Gouveia, C., Kreusch, M., Schmidt, E.C., Marthiellen, M.R., Osorio, L.K.P., Pereira, D.T., Dos Santos, R., Ouriques, L.C., De Paula Martins, R., Latini, A., Ramlov, F., Carvalho, T.J.G., Chow, F., Maraschin, M., Bouzon, Z.L., 2013. The effects of lead and copper on the cellular architecture and metabolism of the red alga Gracilaria domingensis. Microsc. Microanal. 19, 513–524. https://doi.org/10.1017/S1431927613000317.

Habig, W.H., Pabst, M.J., Jakoby, W.B., 1974. Glutathione S-transferases: the first enzymatic step in mercapturic acid formation. J. Biol. Chem. 249, 7130–7139. https://doi.org/10.1016/S0021-9258(19)42083-8.

Hamed, S.M., Selim, S., Klöck, G., Abd Elgawad, H., 2017. Sensitivity of two green microalgae to copper stress: growth, oxidative, and antioxidants analyses. Ecotoxicol. Environ. Saf. 144, 19–25. https://doi.org/10.1016/J.ECOENV.2017.05.048.

Hoffmann, M.A., Nothias, L.-F., Ludwig, M., Fleischauer, M., Gentry, E.C., Witting, M., Dorrestein, P.C., Dührkop, K., Böcker, S., 2021. Assigning confidence to structural annotations from mass spectra with COSMIC. BioRxiv. https://doi.org/10.1101/2021.03.18.435634, 2021.03.18.435634.

Iken, K., Barrera-Oro, E.R., Quartino, M.L., Casaux, R.J., Brey, T., 1997. Grazing by the Antarctic fish *Notothenia coriiceps*: evidence for selective feeding on macroalgae. Antarct. Sci. 9, 386–391. https://doi.org/10.1017/s0954102097000497.

Janknegt, P.J., Marco de Graaff, C., van de Poll, W.H., Visser, R.J.W., Rijstenbil, J.W., Buma, A.G.J., 2009. Short-term antioxidative responses of 15 microalgae exposed to excessive irradiance including ultraviolet radiation. Eur. J. Phycol. 44, 525–539. https://doi.org/10.1080/09670260902943273.

Kaur, M., Saini, K.C., Ojah, H., Sahoo, R., Gupta, K., Kumar, A., Bast, F., 2022. Abiotic stress in algae: response, signaling and transgenic approaches. J. Appl. Phycol. 34, 1843–1869. https://doi.org/10.1007/s10811-022-02746-7.

Koppel, D.J., Adams, M.S., King, C.K., Jolley, D.F., 2019. Diffusive gradients in thin films can predict the toxicity of metal mixtures to two microalgae: validation for environmental monitoring in Antarctic marine conditions. Environ. Toxicol. Chem. 38, 1323–1333. https://doi.org/10.1002/etc.4399.

Liu, J., Li, C., Shi, G., Liu, Y., Du, Z., Ding, M., Gao, S., Xiao, C., Kang, S., Sun, B., 2024. Changes of the trace metals in ice core during 1915–2016 in coastal eastern Antarctica. Adv. Clim. Chang. Res. https://doi.org/10.1016/j.accre.2024.07.003.

Ludwig, M., Nothias, L.F., Dührkop, K., Koester, I., Fleischauer, M., Hoffmann, M.A., Petras, D., Vargas, F., Morsy, M., Aluwihare, L., Dorrestein, P.C., Böcker, S., 2020. Database-independent molecular formula annotation using Gibbs sampling through ZODIAC. Nat. Mach. Intell. 2, 629–641. https://doi.org/10.1038/s42256-020-00234-6.

Machado, M.D., Lopes, A.R., Soares, E.V., 2015. Responses of the alga *Pseudokirchneriella subcapitata* to long-term exposure to metal stress. J. Hazard. Mater. 296, 82–92. https://doi.org/10.1016/J.JHAZMAT.2015.04.022.

Maharana, D., Jena, K., Pise, N.M., Jagtap, T.G., 2010. Assessment of oxidative stress indices in a marine macro brown alga *Padina tetrastromatica* (Hauck) from comparable polluted coastal regions of the Arabian Sea, west coast of India. J. Environ. Sci. 22, 1413–1417. https://doi.org/10.1016/S1001-0742(09)60268-0.

Mallick, N., Mohn, F.H., 2000. Reactive oxygen species: response of algal cells. J. Plant Physiol. 157, 183–193. https://doi.org/10.1016/S0176-1617(00)80189-3.

Marthiellen, M.R., Osorio, L.K.P., Ouriques, L.C., Farias-Soares, F.L., Steiner, N., Kreusch, M., Pereira, D.T., Simioni, C., Costa, G.B., Horta, P.A., Chow, F., Ramlov, F., Maraschin, M., Bouzon, Z.L., Schmidt, É.C., 2014. The effect of cadmium under different salinity conditions on the cellular architecture and metabolism in the red alga *Pterocladiella capillacea* (Rhodophyta, Gelidiales). Microsc. Microanal. 20, 1411–1424. https://doi.org/10.1017/S1431927614012768.

Miller, K.A., Pearse, J.S., 1991. Ecological studies of seaweeds in McMurdo Sound, Antarctica. Integr. Comp. Biol. 31, 35–48. https://doi.org/10.1093/icb/31.1.35.

Momo, F.R., Cordone, G., Marina, T.I., Salinas, V., Campana, G.L., Valli, M.A., Doyle, S. R., Saravia, L.A., 2020. Seaweeds in the Antarctic marine coastal food web. In: Antarctic Seaweeds: Diversity, Adaptation and Ecosystem Services. Springer, pp. 293–307. https://doi.org/10.1007/978-3-030-39448-6_15.

Nakano, Y., Asada, K., 1981. Hydrogen peroxide is scavenged by ascorbate-specific peroxidase in spinach chloroplasts. Plant Cell Physiol. 22, 867–880. https://doi.org/10.1093/oxfordjournals.pcp.a076232.

Navarro, N.P., Mansilla, A., Plastino, E.M., 2010. UVB radiation induces changes in the ultra-structure of *Iridaea cordata*. Micron 41, 899–903. https://doi.org/10.1016/J.MICRON.2010.06.004.

Nothias, L.F., Petras, D., Schmid, R., Dührkop, K., Rainer, J., Sarvepalli, A., Protsyuk, I., Ernst, M., Tsugawa, H., Fleischauer, M., Aicheler, F., Aksenov, A., Alka, O., Allard, P.-M., Barsch, A., Cachet, X., Caraballo, M., Da Silva, R.R., Dang, T., Garg, N., Gauglitz, J.M., Gurevich, A., Isaac, G., Jarmusch, A.K., Kameník, Z., Kang, K.B., Kessler, N., Koester, I., Korf, A., Le Gouellec, A., Ludwig, M., Christian, M.H., McCall, L.-I., McSayles, J., Meyer, S.W., Mohimani, H., Morsy, K., Moyne, A.R., Neumann, K.M., Neuweger, B.A., Nguyen, F., Nothias-Esposito, H.R., Paolini, L., Phelan, B.S., Pluskal, M., Quinn, M., Rogers, T., Shrestha, J., Tripathi, E., van der Hooft, B.P., Vargas, J., Weldon, J.L., Witting, M.R., Yang, T., Zhang, R., Zubeil, H.M., Kohlbacher, N., Böcker, S., Alexandrov, T., Bandeira, J., Dorrestein, P.-C., 2020. Feature-based molecular networking in the GNPS analysis environment. Nat. Methods 17, 905–908. https://doi.org/10.1038/s41592-020-0933-6.

Nowicka, B., 2022. Heavy metal–induced stress in eukaryotic algae—mechanisms of heavy metal toxicity and tolerance with particular emphasis on oxidative stress in exposed cells and the role of antioxidant response. Environ. Sci. Pollut. Res. 29, 16860–16911. https://doi.org/10.1007/s11356-021-18419-w.

Pacchini, S., Piva, E., Schumann, S., Irato, P., Pellegrino, D., Santovito, G., 2023. An experimental study on antioxidant enzyme gene expression in *Trematomus newnesi* (Boulenger, 1902) experimentally exposed to perfluoro-octanoic acid. Antioxidants 12, 352. https://doi.org/10.3390/ANTIOX12020352/S1.

Pinto, E., Sigaud-Kutner, T.C.S., Leitão, M.A.S., Okamoto, O.K., Morse, D., Colepicolo, P., 2003. Heavy metal–induced oxidative stress in algae. J. Phycol. 39, 1008–1018. https://doi.org/10.1111/j.0022-3646.2003.02-193.x.

Pueschel, C.M., 1990. Cell structure. In: Cole, K.M., Sheath, R.G. (Eds.), Biology of the Red Algae. Cambridge University Press, Cambridge, pp. 7–42.

Ralph, P.J., Smith, R.A., MacInnis-Ng, C.M.O., Seery, C.R., 2007. Use of fluorescence-based ecotoxicological bioassays in monitoring toxicants and pollution in aquatic systems: review. Toxicol. Environ. Chem. 89, 589–607. https://doi.org/10.1080/02772240701561593.

Rezayian, M., Niknam, V., Ebrahimzadeh, H., 2019. Oxidative damage and antioxidative system in algae. Toxicol. Rep. 6, 1309–1313. https://doi.org/10.1016/J.TOXREP.2019.10.001.

Runcie, J.W., Townsend, A.T., Seen, A.J., 2009. The application of lead isotope ratios in the Antarctic macroalga *Iridaea cordata* as a contaminant monitoring tool. Mar. Pollut. Bull. 58, 961–966. https://doi.org/10.1016/j.marpolbul.2009.03.010.

Santovito, G., Piccinni, E., Boldrin, F., Irato, P., 2012. Comparative study on metal homeostasis and detoxification in two Antarctic teleosts. Comp. Biochem. Physiol. C Toxicol. Pharmacol. 155, 580–586. https://doi.org/10.1016/J.CBPC.2012.01.008.

Schelbert, S., Aubry, S., Burla, B., Agne, B., Kessler, F., Krupinska, K., Hörtensteiner, S., 2009. Pheophytin pheophorbide hydrolase (pheophytinase) is involved in chlorophyll breakdown during leaf senescence in Arabidopsis. Plant Cell 21, 767–785. https://doi.org/10.1105/TPC.108.064089.

Schmid, R., Heuckeroth, S., Korf, A., Smirnov, A., Myers, O., Dyrlund, T.S., Bushuiev, R., Murray, K.J., Hoffmann, N., Lu, M., Sarvepalli, A., Zhang, Z., Fleischauer, M., Dührkop, K., Wesner, M., Hoogstra, S.J., Rudt, E., Mokshyna, O., Brungs, C., Ponomarov, K., Mutabdžija, L., Damiani, T., Pudney, C.J., Earll, M., Helmer, P.O., Fallon, T.R., Schulze, T., Rivas-Ubach, A., Bilbao, A., Richter, H., Nothias, L.F., Wang, M., Orešič, M., Weng, J.K., Böcker, S., Jeibmann, A., Hayen, H., Karst, U., Dorrestein, P.C., Petras, D., Du, X., Pluskal, T., 2023. Integrative analysis of multimodal mass spectrometry data in MZmine 3. Nat. Biotechnol. 41, 447–449. https://doi.org/10.1038/s41587-023-01690-2.

Schmidt, É.C., Scariot, L.A., Rover, T., Bouzon, Z.L., 2009. Changes in ultrastructure and histochemistry of two red macroalgae strains of *Kappaphycus alvarezii* (Rhodophyta, Gigartinales), as a consequence of ultraviolet B radiation exposure. Micron 40, 860–869. https://doi.org/10.1016/J.MICRON.2009.06.003.

Schumann, S., Mozzi, G., Piva, E., Devigili, A., Negrato, E., Marion, A., Bertotto, D., Santovito, G., 2023. Social buffering of oxidative stress and cortisol in an endemic cyprinid fish. Sci. Rep. 13, 1–12. https://doi.org/10.1038/s41598-023-47926-8.

Silva, S.G., Paula, P., da Silva, J.P., Mil-Homens, D., Teixeira, M.C., Fialho, A.M., Costa, R., Keller-Costa, T., 2022. Insights into the antimicrobial activities and metabolomes of aquimarina (Flavobacteriaceae, Bacteroidetes) species from the rare marine biosphere. Mar. Drugs 20, 423. https://doi.org/10.3390/md20070423.

Sumner, L.W., Amberg, A., Barrett, D., Beale, M.H., Beger, R., Daykin, C.A., Fan, T.W.M., Fiehn, O., Goodacre, R., Griffin, J.L., Hankemeier, T., Hardy, N., Harnly, J., Higashi, R., Kopka, J., Lane, A.N., Lindon, J.C., Marriott, P., Nicholls, A.W., Reily, M. D., Thaden, J.J., Viant, M.R., 2007. Proposed minimum reporting standards for chemical analysis: Chemical Analysis Working Group (CAWG) Metabolomics Standards Initiative (MSI). Metabolomics 3, 211–221. https://doi.org/10.1007/S11306-007-0082-2.

Tolomeo, A.M., Carraro, A., Bakiu, R., Toppo, S., Place, S.P., Ferro, D., Santovito, G., 2016. Peroxiredoxin 6 from the Antarctic emerald rockcod: molecular characterization of its response to warming. J. Comp. Physiol. B 186, 59–71. https://doi.org/10.1007/S00360-015-0935-3.

Wang, M., Carver, J.J., Phelan, V.V., Sanchez, L.M., Garg, N., Peng, Y., Nguyen, D.D., Watrous, J., Kapono, C.A., Luzzatto-Knaan, T., Porto, C., Bouslimani, A., Melnik, A. V., Meehan, M.J., Liu, W.T., Crüsemann, M., Boudreau, P.D., Esquenazi, E., Sandoval-Calderón, M., Kersten, R.D., Pace, L.A., Quinn, R.A., Duncan, K.R., Hsu, C. C., Floros, D.J., Gavilan, R.G., Kleigrewe, K., Northen, T., Dutton, R.J., Parrot, D., Carlson, E.E., Aigle, B., Michelsen, C.F., Jelsbak, L., Sohlenkamp, C., Pevzner, P., Edlund, A., McLean, J., Piel, J., Murphy, B.T., Gerwick, L., Liaw, C.C., Yang, Y.L., Humpf, H.U., Maansson, M., Keyzers, R.A., Sims, A.C., Johnson, A.R., Sidebottom, A. M., Sedio, B.E., Klitgaard, A., Larson, C.B., Boya, C.A.P., Torres-Mendoza, D., Gonzalez, D.J., Silva, D.B., Marques, L.M., Demarque, D.P., Pociute, E., O'Neill, E.C., Briand, E., Helfrich, E.J.N., Granatosky, E.A., Glukhov, E., Ryffel, F., Houson, H., Mohimani, H., Kharbush, J.J., Zeng, Y., Vorholt, J.A., Kurita, K.L., Charusanti, P., McPhail, K.L., Nielsen, K.F., Vuong, L., Elfeki, M., Traxler, M.F., Engene, N., Koyama, N., Vining, O.B., Baric, R., Silva, R.R., Mascuch, S.J., Tomasi, S., Jenkins, S., Macherla, V., Hoffman, T., Agarwal, V., Williams, P.G., Dai, J., Neupane, R., Gurr, J., Rodríguez, A.M.C., Lamsa, A., Zhang, C., Dorrestein, K., Duggan, B.M., Almaliti, J., Allard, P.M., Phapale, P., Nothias, L.F., Alexandrov, T., Litaudon, M., Wolfender, J. L., Kyle, J.E., Metz, T.O., Peryea, T., Nguyen, D.T., VanLeer, D., Shinn, P., Jadhav, A., Müller, R., Waters, K.M., Shi, W., Liu, X., Zhang, L., Knight, R., Jensen, P.R., Palsson, B., Pogliano, K., Linington, R.G., Gutiérrez, M., Lopes, N.P., Gerwick, W.H., Moore, B.S., Dorrestein, P.C., Bandeira, N., 2016. Sharing and community curation of mass spectrometry data with Global Natural Products Social Molecular Networking. Nat. Biotechnol. 34, 828–837. https://doi.org/10.1038/nbt.3597.

Wiencke, C., Clayton, M.N., 2002. Antarctic seaweeds. In: Gantner Verlag, A.R.G. (Ed.), Synopses of the Antarctic Benthos. Ruggell, Liechtenstein. doi:10.2/jquery.min.js.

Xia, J.R., Li, Y.J., Lu, J., Chen, B., 2004. Effects of copper and cadmium on growth, photosynthesis, and pigment content in *Gracilaria lemaneiformis*. Bull. Environ. Contam. Toxicol. 73, 979–986. https://doi.org/10.1007/S00128-004-0522-X.

Zhang, W., Tan, N.G.J., Li, S.F.Y., 2013. NMR-based metabolomics and LC-MS/MS quantification reveal metal-specific tolerance and redox homeostasis in *Chlorella vulgaris*. Mol. Biosyst. 10, 149–160. https://doi.org/10.1039/c3mb70425d.

Zhu, X., Zou, D., Huang, Y., Cao, J., Sun, Y., Chen, B., Chen, X., 2017. Physiological responses of Porphyra haitanensis (Rhodophyta) to copper and cadmium exposure. Bot. Mar. 60, 27–37. https://doi.org/10.1515/BOT-2016-0117.